Chemical Engineering Journal 150 (2009) 8–14

Contents lists available at ScienceDirect

Chemical Engineering Journal

journal homepage: www.elsevier.com/locate/cej

Pd/γ-Al_2O_3 monolithic catalysts for NO_x reduction with CH_4 in excess of O_2: Effect of precursor salt

J.C. Martín [a], S. Suarez [b], M. Yates [a], P. Ávila [a,*]

[a] Instituto de Catálisis y Petroleoquímica, C.S.I.C. c/Marie Curie n°2, Madrid 28049, Spain
[b] CIEMAT-PSA Avda. Complutensen°22, Madrid 28040, Spain

ARTICLE INFO

Article history:
Received 21 July 2008
Received in revised form
14 November 2008
Accepted 19 November 2008

Keywords:
Nitrogen oxide removal
$DeNO_x$
HC-SCR
Pd Catalysts
Monolithic catalysts
Methane-SCR
Palladium precursors

ABSTRACT

Palladium monolithic catalysts based on γ-Al_2O_3 were developed and their activities and selectivities for the selective catalytic reduction of nitrogen oxides employing methane as the reducing agent in oxygen excess (CH_4-SCR) for use at pilot plant scale, were determined. The alumina monoliths were sulphated to increase the activity of the support and subsequently impregnated with one of three precursor salts: palladium chloride, nitrate or acetate, respectively. The catalysts were characterised by XRF, XRD, TGA–DTA, H_2-TPR, N_2 ad/desorption and MIP. Significant differences in the catalytic activities, selectivity and stabilities were found. In the case of nitrate and acetate palladium precursors, multilayer sulphates for both and $Al_2(SO_4)$ phase for the latter were observed that may inhibit the interaction of the reactants with the active phase, leading to catalysts with reduced activity. Palladium chloride was the most efficient precursor for NO_x abatement, not only due to the stability of the surface sulphates that hinder the competitive CH_4 oxidation reaction but also to the presence of Cl^- ions that seem to play an important role in the reaction. This catalyst had the lowest tendency for the competing hydrocarbon oxidation reaction and also demonstrated the highest stability after 40 h of reaction in the chosen operating conditions.

1. Introduction

The elimination of nitrogen oxides from stationary source effluent gases is a legal requirement in many industrialised countries. Although various systems have been developed depending on the particular application, selective catalytic reduction of NO_x with ammonia (SCR process) is still the most common technology in use. Nevertheless, in recent years SCR of NO_x with hydrocarbons in lean conditions has been extensively studied, in principle for the decontamination of mobile source exhaust gases employing part of the fuel as the reducing agent. These studies have led to significant progress in the understanding of the process. However, difficulties encountered in reaching the desired levels of activity, selectivity and stability has lead to the application of this technology to be directed towards the purification of NO_x emissions from stationary sources. In this field the use of methane as the reducing agent for the abatement of NO_x according to Eq. (1) presents a series of advantages in terms of cost and availability due to it being the principal component of natural gas which is usually present in many combustion plants [1–4]:

$$2NO + CH_4 + O_2 \rightarrow N_2 + 2H_2O + CO_2 \quad (1)$$

The most promising catalysts were initially those based on zeolites, thought to be due to their acid character [5,6]. In order to create acid properties similar to those present in zeolites the use of alumina with adequate pretreatment could be an attractive alternative. It has been demonstrated that sulphated alumina (Al_2O_3/SO_4^{2-}) prepared from γ-alumina has superacid character $Ho \leq -14.5$ [7].

For the CH_4-SCR noble metals such as Pt, Pd and Rh among others have been employed as active phases [8–10], as too metal oxides such as Co, Fe or Cu [11] but in general the noble metals had higher activities than the metal oxides. An important drawback of Pt-based catalysts is the low N_2 selectivity with N_2O being one of the principle reaction products [12,13]. Due to its high methane combustion values Pd is a widely used noble metal in the three-way catalyst (TWC) formulation, however, its catalytic activity can be controlled by the synthesis method employed. Thus, Pd catalysts may vary from being inactive to very active, depending on the catalysts design [14]. Loughran and Resasco [15] studied Pd catalysts for the reduction of NO_x with CH_4 concluding that the acid properties of the support had an important effect on the catalytic activity. The use of Pd supported on acidic materials was correlated with the stabilisation of Pd^{2+} species which have low activity for methane oxidation [14].

In previous work the properties of γ-Al_2O_3 based monolithic support treated with mineral acids of different acid strengths were studied. The results showed that pretreatment of a Co/γ-Al_2O_3 catalysts with H_2SO_4 led to the highest NO conversions, related to the

* Corresponding author. Tel.: +34 915854799; fax: +34 915854760.
E-mail address: pavila@icp.csic.es (P. Ávila).

1385-8947/$ – see front matter © 2009 Elsevier B.V. All rights reserved.
doi:10.1016/j.cej.2008.11.050

strong acid sites that stabilised Co^{2+} species [16]. In this study we have explored the catalytic properties of Pd catalyst conformed as a monolithic γ-Al_2O_3 structure that had been pretreated with H_2SO_4 (γ-Al_2O_3/SO_4^{2-}). The effect of the palladium precursor salt was evaluated by employing different counter anions: nitrate, chloride or acetate. The results are discussed in terms of the textural properties (MIP, N_2 ad/desorption), crystal phases (XRD) and types of sulphur species (TGA, and TPR-H_2). The catalytic performance in the SCR reaction of NO with CH_4 in O_2 excess was analysed considering the effect of the temperature, competitive methane oxidation reaction and the catalysts stability with time in reaction.

2. Experimental

2.1. Catalyst preparation

Alumina monoliths of 64 cells (8×8), a wall thickness of 0.50 mm, open channel width of 1.73 mm that leads to a cell density of 14.9 cells/cm^2 and geometric surface area of 1189 m^2/m^3, were prepared by kneading a commercial boehmite alumina, Pural SB from Sasol, with deionised water and organic temporary additives to achieve the required rheological properties for its subsequent extrusion. Once extruded the monoliths were dried at ambient temperature then subsequently calcined at 600 °C for 4 h. This monolithic support is denominated as A (γ-Al_2O_3 monolith).

The γ-Al_2O_3 monolith was sulphated as previously described by Li et al. (for powdered catalysts) [17], impregnating the monolith with a 2.5 molar aqueous solution of H_2SO_4 for 30 min, while the monolith was continuously moved in up and down within the solution to ensure a homogeneous coverage that reached 18 wt.% of sulphate. Subsequently, the monoliths were dried at ambient temperature, then at 110 °C for 12 h and finally heat-treated at 600 °C for 4 h. The support thus obtained was designated as SA (sulphated alumina monolith).

Precursors of the Pd active phase were incorporated by an impregnation method using either aqueous solutions of palladium II nitrate ($Pd(NO_3)_2{\cdot}XH_2O$, 99.9 wt.% from Alfa Æsar), palladium II chloride ($PdCl_2$ 99.9 wt.% from Johnson Matthey) or acetone (99.9% from Johnson Matthey) as the solvent in the case of palladium (II) acetate ($Pd(OAc)_2$ from Hexakis with a 47.14 wt.% of Pd). The solids were subsequently dried at ambient temperature then calcined at 600 °C for 4 h. In all cases the concentration of Pd deposited on the sulphated γ-alumina monolith was maintained at between 0.1 and 0.17 wt.%, the variation in the final amounts being due to loss of some of the active phase during the subsequent calcination steps. The catalysts thus obtained were denominated as Pd–Cl/SA, Pd–N/SA and Pd–Ac/SA.

2.2. Characterisation

The palladium content of the catalysts was determined by *X-ray fluorescence* using a Seifert EXTRA-II spectrometer, equipped with two fine focus X-ray lines, Mo and W anodes a Si(Li) detector with an active area of 80 mm^2 and a resolution of 157 eV at 5.9 keV (Mn Kα).

The crystal phases were studied by *X-ray diffraction* (XRD) employing a Seifert 3000P diffractometer on powdered samples working at 40 kV and 25 mA. The incident radiation was of copper Kα_1 with a wave length of $\lambda = 1.5406$ nm, with a nickel filter. The diffractograms were obtained in the $2\theta = 10$–80° range with steps of 0.02° at a rate of 2 s per step. The identification of the crystalline phases was made using the RAYFLEX-Analyze 2.25 software.

Thermal gravimetric analyses of the samples were carried out on a Netzsch 409 EP simultaneous thermal analysis device. The TGA–DSC curves were measured using approximately 20–30 mg of powered sample in an air flow of 75 ml min^{-1} at a rate of 5 °C min^{-1} from room temperature to 1000 °C, using α-alumina as reference.

Temperature-programmed reduction (TPR) experiments were carried out with a Micromeritics TPD/TPR 2900 apparatus equipped with a thermal conductivity detector. Reduction profiles were obtained on samples of approximately 30 mg, in a gas flow of 10% H_2/Ar at a rate of 50 mL(STP)min^{-1}. The temperature was increased from ambient to 1000 °C at a rate of 10 °C min^{-1} with the amount of hydrogen consumed determined as a function of temperature.

Mercury intrusion porosimetry (MIP) analyses were employed to determine the pore size distribution and pore volume over the range of approximately 100 μm down to 7.5 nm diameter, utilising CE Instruments Pascal 140/240 apparatus, on samples previously dried overnight at 150 °C. Approximately 0.2 g of sample was accurately weighed into the sample holder that was subsequently outgassed at room temperature for 5 min to a vacuum of <10 Pa before filling with mercury and starting the analysis. The pressure/volume data were analysed by use of the Washburn Equation [18] assuming a cylindrical non-intersecting pore model, taking the recommended values for the mercury contact angle of 141° and surface tension 484 mN m^{-1} [19].

The *specific surface area* and pore size distribution in the micro- (0–2 nm) and meso-pore (2–50 nm) diameter ranges were determined by nitrogen ad/desorption isotherms measured with a Carlo Erba Sorptomatic 1800 on samples previously outgassed overnight at 300 °C to a vacuum of >0.1 Pa. The specific surface areas of the samples (S_{BET}) were determined by the BET method from the corresponding nitrogen adsorption isotherm. Combination of the nitrogen adsorption and mercury porosimetry results leads to the determination of the total pore volume of the conformed materials.

The *mechanical strengths* of the monoliths were determined using a Chatillon LTCM Universal Tensile Compression and Spring Tester with a test head of 0.73 mm diameter. The test head was positioned over one of the channel walls of the monolith and the pressure slowly increased until rupture of the wall was caused. The average of 10 measurements was taken for each material to ensure the precision of the result.

2.3. Catalytic activity

The catalytic activities of the materials were determined in a stainless steel tubular flow reactor 85 cm in length with an internal diameter of 3.5 cm, operating in an isothermal integral regime. The monolithic samples of 64 channels and 10 cm in length were placed in the reactor with the space between the sample and the reactor wall being filled with alumina wool and carborundum, both inert in the reaction, to ensure that the gas mixture passed through the open channels of the monolith.

For the determination of the catalytic activities of the samples the following conditions were chose: total flow $Q = 3500$ ml min^{-1}, temperature = 300–600 °C, $P = 120$ kPa, $GHSV_{(N.C.)} = 7000$ h^{-1}, $v_L = 0.39$ mN s^{-1}. The feed gas concentrations were: [NO] = 500 ppm, [CH_4] = 1000 ppm, [O_2] = 5 vol.%, and N_2 balance. The concentrations at the reactor inlet and outlet were determined by N_2 quimiluminescence for NO, NO_2 and NO_x in a Signal Series 4000VM NO_x Analyser. The CH_4 concentration was measured by a Horiba THC FIA-510 flame ionisation detector (FID) and the formation of CO_2 was monitored by IR spectroscopy in a Horiba VIA-510 Analyser.

3. Results and discussion

It has been shown that the optimum Pd loading on an alumina support with a surface area of 136 m^2 g^{-1} to achieve the maximum NO conversion was about 0.1 wt.%, while at higher contents (1 wt.%)

Table 1
Textural and mechanical properties of the Pd/Al_2O_3 monoliths.

Designation	Support composition	Pd (wt.%)	SO_4^{2-} (wt.%)	Surface area S_{BET} ($m^2\,g^{-1}$)	Total pore volume ($cm^3\,g^{-1}$)	Mesopore volume ($cm^3\,g^{-1}$)	Macropore volume ($cm^3\,g^{-1}$)	Mechanical strength ($kg\,cm^{-2}$)
A	Al_2O_3	–	–	220	0.80	0.65	0.15	215
Pd–Cl/A	Al_2O_3	0.15	–	219	0.88	0.59	0.21	144
SA	SO_4^{2-}/Al_2O_3	–	18.0	201	0.73	0.59	0.14	191
Pd–Cl/SA	SO_4^{2-}/Al_2O_3	0.13	8.4	215	0.91	0.58	0.32	190
Pd–N/SA	SO_4^{2-}/Al_2O_3	0.11	8.6	200	0.85	0.53	0.32	71
Pd–Ac/SA	SO_4^{2-}/Al_2O_3	0.17	17.0	159	0.62	0.35	0.27	24

A: γ-Al_2O_3 monolithic support and SA: SO_4^{2-}/γ-Al_2O_3 monolithic support. (Selected catalyst in bold.)

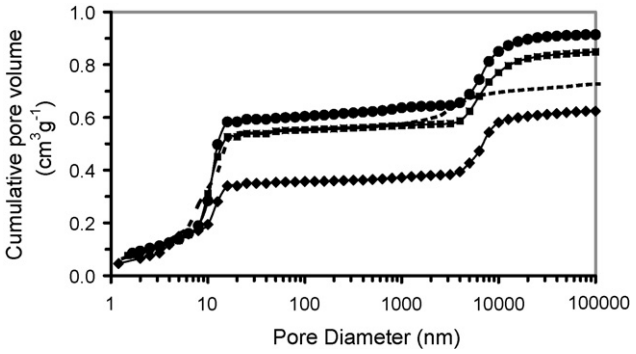

Fig. 1. Cumulative pore volume curves of sulphated alumina support and catalysts. Data obtained from combination of nitrogen ad/desorption isotherms and mercury intrusion porosimetry: (– – –) SA; (○) Pd–Cl/SA; (■) Pd–N/SA; (×) Pd–Ac/SA.

the methane oxidation reaction was promoted and the catalytic activity was severely reduced [20]. Thus, in these supports with specific surface areas of approximately 200 $m^2\,g^{-1}$ Pd loadings close to 0.2 wt.% were produced. At higher Pd loadings the slight increase in the NO_x conversion activity would not justify the corresponding increases in the final cost of the catalyst [21]. In Table 1 the textural and mechanical properties of the original γ-Al_2O_3 monolith support, sulphated support and Pd catalysts are collated.

The total porosities and pore size distributions of the samples were analysed by combining the data obtained from the nitrogen isotherms with the corresponding data obtained from MIP for which the cumulative pore volume curves plotted against pore diameter are shown in Fig. 1. The γ-Al_2O_3 monolith gave rise to a bimodal pore size distribution in the mesopore region with peak maxima at about 4 and 11 nm, due to the mesoporous nature of the alumina and a further porosity in pores of about 2-5 μm due to the interparticulate porosity. The position of this macroporosity is directly related to the primary particle size of the alumina [22]. Sulphidation of this support caused a slight reduction in both the macro and mesopores and the specific surface area due to deposition of the sulphate species in addition to a slight reduction in the mechanical strength due to the widening of the macropores due to the acid attack.

Different behaviours were observed depending on the active phase precursor salts selected for the impregnation process since this removed some of the sulphate species, increasing both the volume and width of the macropores that generally reduced still further the mechanical strengths. Thus, treatment with sulphuric acid slightly reduced the specific surface area and mesopore volume compared to the alumina support but although the macropore volume was similar to the original support the pores were wider due to the acid attack that also caused a slight decrease in the mechanical strength. Impregnation of the Pd active phase with the chloride precursor led to a slight rise in the specific surface area and total pore volume compared to the sulphated support, probably due to the lixiviation of some sulphate species during the impregnation procedure, although the mechanical strength was unaffected. A similar increase in the wider pores was observed for the sample impregnated with the nitrate precursor, although the surface area remained unchanged compared to the sulphated support but the mechanical strength displayed a marked reduction. For the sample prepared with the acetate precursor there was a significant decrease in the mesopore volume along with a slight increase in the macroporosity that led to significant decreases in both the specific surface area and the mechanical strength. These results indicated that the impregnation route using an acetate salt in acetone led to blocking of the narrower pores maybe caused by migration of the sulphate species in this media.

Although significant modifications in the total porosities and mechanical strengths were observed after the incorporation of the active phase, no effects on the crystallinity of the alumina were observed by XRD (Fig. 2). However, for the monolith impregnated with acetate, Pd–Ac/SA, a diffraction peak at $2\theta \sim 26^\circ$ corresponding to an $Al_2(SO_4)_3$ phase was detected. This result indicated that the reduction of the pore volume was mainly due to the formation of this aluminium sulphate phase.

Surface sulphur containing species may have a variety of structures: sulphates, sulphites, bisulphates, monodentates and polydentates depending on the support, sulphate concentration, synthesis process, presence of water and the heat treatment temperature. Three general sulphates species on Al_2O_3/SO_4^{2-} prepared with different sulphate loadings have been identified by thermal analysis and corroborated by FTIR-pyridine, XPS and TPD-NH_3 [23]. In that study the authors demonstrated that thermal analysis allowed the identification of these different sulphate species present on the alumina samples. At low sulphate concentrations (H_2SO_4 < 0.8 M) only a decomposition peak at 950 °C was observed. From H_2SO_4 concentration between 0.8 and 2.4 M, a second peak

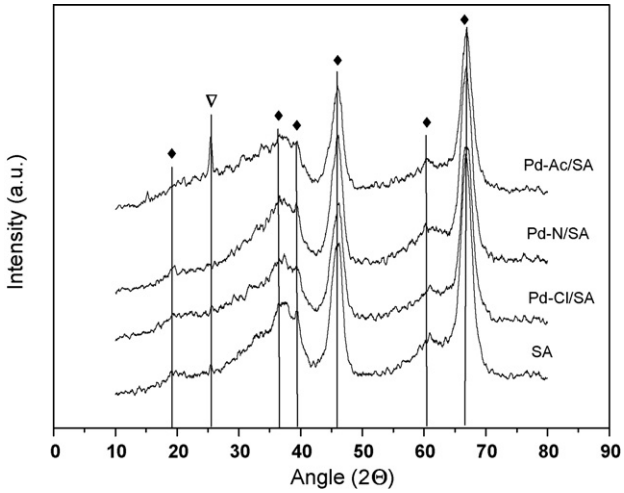

Fig. 2. X-ray diffraction patterns obtained with the sulphated support and the Pd catalysts before reaction: (▽) $Al_2(SO_4)_3$ and (♦) γ-Al_2O_3.

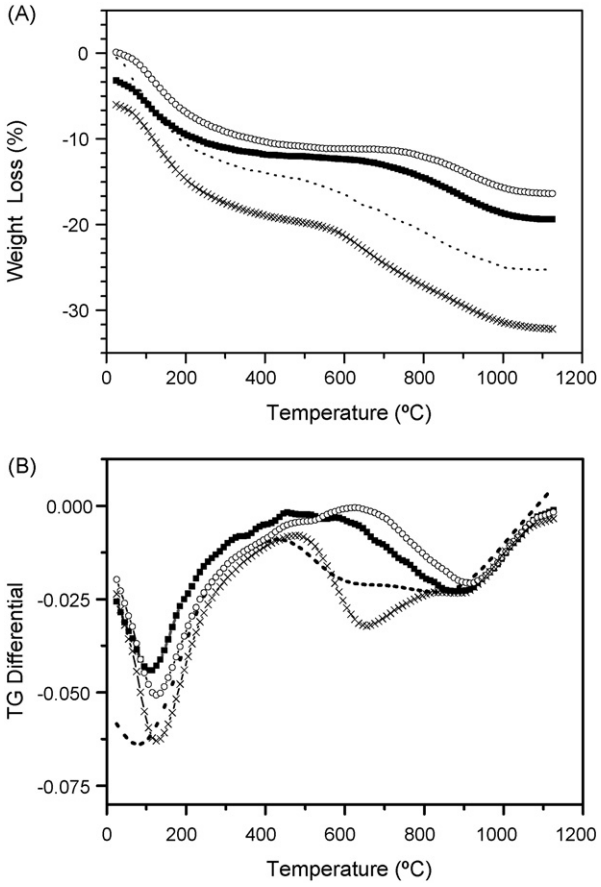

Fig. 3. Thermogravimetric analysis (TGA) (A) and differential thermal gravimetry (DTG) (B) curves for the sulphated support and Pd catalysts before reaction: (– – –) SA; (◯) Pd–Cl/SA; (■) Pd–N/SA; (×) Pd–Ac/SA.

at 630 °C was observed while above 2.4 M a third peak at 800 °C appeared at similar temperature to the decomposition temperature for pure $Al_2(SO_4)_3$. The peaks at 950, 630, and 800 °C were assigned to the decomposition of surface sulphate, amorphous multilayer sulphate and crystallised $Al_2(SO_4)_3$, respectively. Surface sulphate induced Lewis superacid sites, multilayer sulphates created weaker Brönsted acid sites and the crystallised $Al_2(SO_4)_3$ was neutral.

The thermogravimetric and differential thermal analysis results for the sulphated support and the three catalysts are presented in Fig. 3A and B, respectively. These results have been normalised by the sample weight and in Fig. 3A the curves corresponding to Pd–N/SA and Pd–Ac/SA offset in the vertical axis in order to more easily appreciate the differences between the curves. From these graphs the initial weight loss with a maximum close to 100 °C corresponds to the loss of physisorbed water. The weight losses above 600 °C were due to the loss of the sulphate species. It should be noted that the weight losses above 600 °C were similar for the sulphated alumina and the sample prepared with the acetate precursor, in accordance with the sulphate contents in Table 1. Similarly, the weight losses observed for the samples produced from the chloride and nitrate precursors were much lower, as expected from their sulphate loadings given in Table 1.

From analysis of the DTG curves above 500 °C it may be observed that the sulphated alumina support was characterised by a wide band with two maxima centred at about 620 and 900 °C. Thus, these peaks were assigned to multilayer and surface sulphate species, respectively. The catalysts prepared from the chloride and nitrate salts gave rise to a peak with a maximum located around 900 °C

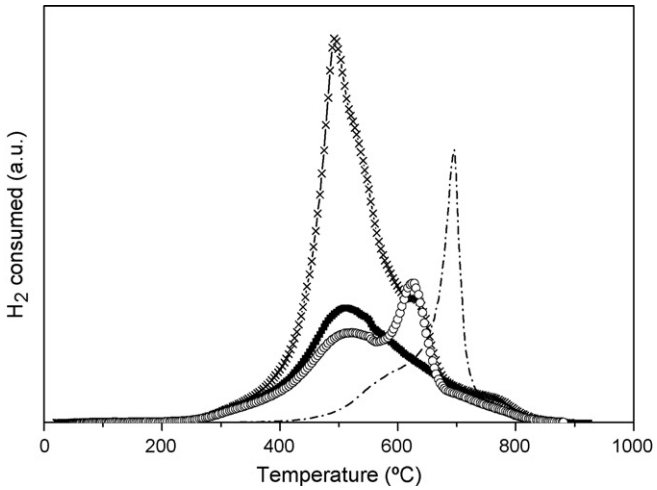

Fig. 4. H_2-TPR curves for the sulphated support and the Pd catalysts: (- - - -) SA; (◯) Pd–Cl/SA; (■) Pd–N/SA; (×) Pd–Ac/SA. TPR conditions: $Q = 50\ mL\ min^{-1}$ (10% H_2/Ar). Temperature programme: r.t. to 1000 °C at a rate of 10 °C min^{-1}.

related to strongly anchored surface sulphate species with Lewis character. Compared to sulphated alumina, the contribution at 620 °C was practically non-existent, suggesting the elimination of the multilayer sulphate species during the impregnation process. In the case of the catalyst prepared with the acetate precursor the intensity of the band centred at 650 °C was considerably higher than that of the sulphated support, suggesting that in part this signal was due to the decomposition of the $Al_2(SO_4)_3$ phase observed by XRD for this material. The presence of these multilayer sulphates could inhibit the access of the effluent gases to be treated to the strong acid sites of the sulphated alumina.

The sulphate species in the sulphated support and the three catalysts were also studied by temperature programme reduction with hydrogen. From the results shown in Fig. 4 it may be observed that for the sulphated support there were two bands of hydrogen consumption corresponding to the reduction of the two types of sulphate. The first peak observed at about 580 °C was probably due to multilayer sulphate species, while the second more intense peak at about 700 °C corresponded to the surface sulphate.

From the literature reduction peaks corresponding to PdO particles are observed at temperatures below 50 °C [24] although in some cases a peak appears at 300 °C due to PdO that strongly interacts with the support [25]. However, with the materials studied here no peaks related to PdO could be identified in the TPR curves, probably in part due to the low Pd loadings. In comparison for the curve obtained with the sulphated support it should be noted that impregnation with Pd lowered the reduction temperature for the sulphate species by around 80 °C. Thus, the Pd–Cl/SA sample presented the highest amount of species related to Lewis acid sites corresponding to the peak centred at about 620 °C. For the Pd–N/SA material the peak associated with surface sulphates was greater than that observed for the sample made from the chloride precursor but that associated with Lewis acidity was much lower. For the material produced from the acetate precursor the hydrogen consumption due to Lewis acidity was similar to that observed for the Pd–Cl/SA sample. However, for this sample the peak maxima close to 500 °C and the shoulder at 520 °C due to multilayer sulphates and $Al_2(SO_4)_3$, respectively, were much higher than the other three samples, in accordance with the XRD results.

The NO reductions with CH_4 in O_2 excess for the Pd catalysts as a function of the reaction temperature are presented in Fig. 5. In the reaction products no NO_2, N_2O or NH_3 were detected. It may be seen from the figure that all the catalytic activity curves passed through a maximum at a temperature that depended on the precursor salt.

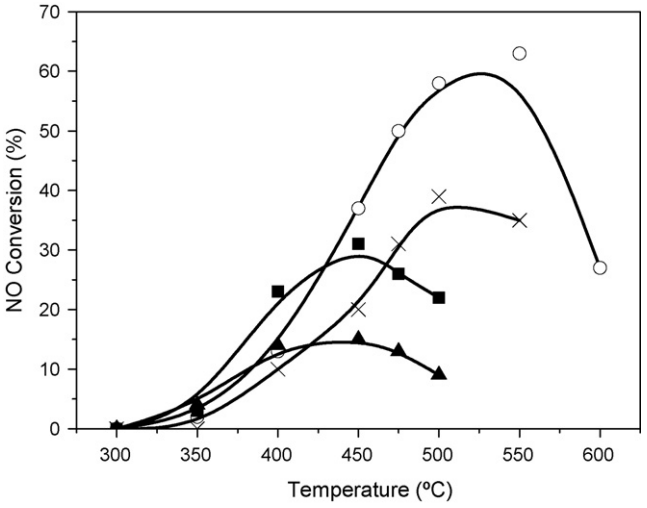

Fig. 5. Variation of the NO conversion with temperature for Pd catalysts: (▲) Pd/A; (◯) Pd–Cl/SA; (■) Pd–N/SA; (×), Pd–Ac/SA. Operating conditions: total flow $Q = 3500\,mL\,min^{-1}$, $T = 300–600\,^{\circ}C$, $P = 120\,kPa$, $GHSV_{(N.C.)} = 7000\,h^{-1}$, and $v_L = 0.39\,mN\,s^{-1}$. Gas feed composition: [NO] = 500 ppm, [CH_4] = 1000 ppm, [O_2] = 5 vol.%, and [N_2] = balance.

All the catalysts prepared with the Al_2O_3/SO_4^{2-} support exhibited a clear improvement in the catalytic activity compared to the Pd/A catalyst that had a maximum NO conversion of less than 15%. The Pd-Cl/SA catalyst was the most active of the series, reaching conversion values of around 70% at 550 °C under the chosen reaction conditions. The maximum NO conversion of 33 and 38% for the catalysts prepared from nitrate and acetate precursors were attained at 450 and 500 °C, respectively.

An important aspect that limits the NO conversion activity of these catalysts in lean conditions is the competitive methane oxidation reaction. In Figs. 6 and 7 the behaviour of these catalysts for methane oxidation are shown in the presence and absence of NO, respectively. In Fig. 6 the amount of methane oxidised in the presence of NO was estimated from the difference between the total CH_4 reacted and that required for the reaction with NO according to the stochiometry shown in Eq. (1). The methane oxidation activities displayed the opposite trend to that observed for NO reduction. The temperature at which the maximum NO reduction was attained coincided with the point at which 50% of the CH_4 was oxidised, following the order: Pd–N/SA < Pd–Ac/SA < Pd–Cl/SA. In agreement

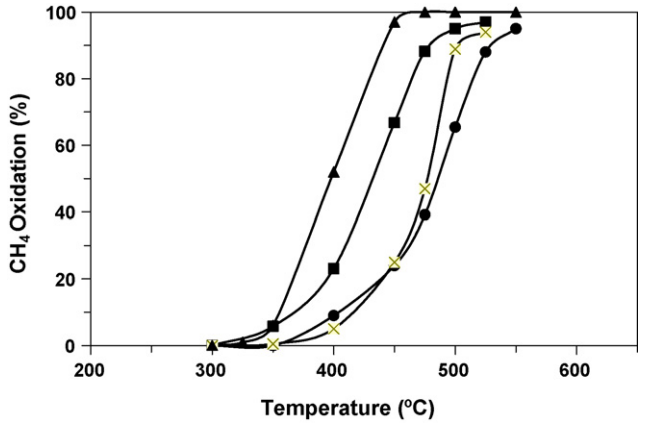

Fig. 6. CH_4 combustion for $NO + CH_4 + O_2$ versus temperature for the Pd catalysts: (▲) Pd/A; (●) Pd–Cl/SA; (■) Pd–N/SA; (×) Pd–Ac/SA. Operating conditions: total flow $Q = 3500\,mL\,min^{-1}$, $T = 300–600\,^{\circ}C$, $P = 120\,kPa$, $GHSV_{(N.C.)} = 7000\,h^{-1}$, and $v_L = 0.39\,mN\,s^{-1}$. Gas feed composition: [NO] = 0–500 ppm, [CH_4] = 1000 ppm, [O_2] = 5 vol.%, and [N_2] = balance.

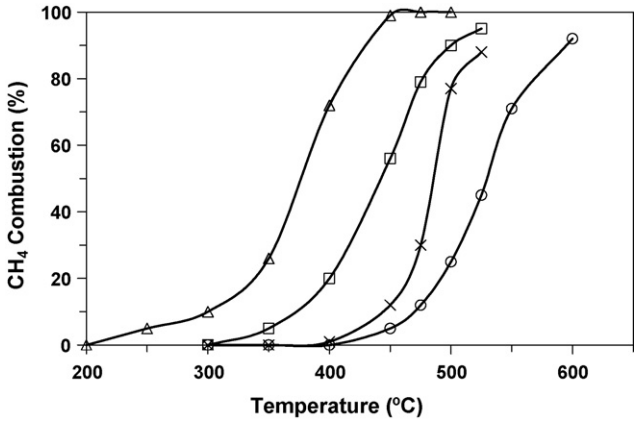

Fig. 7. CH_4 combustion for $CH_4 + O_2$ versus temperature for the Pd catalysts: (△) Pd/A; (◯) Pd–Cl/SA; (□) Pd–N/SA; (×) Pd–Ac/SA. Operating conditions: total flow $Q = 3500\,mL\,min^{-1}$, $T = 300–600\,^{\circ}C$, $P = 120\,kPa$, and $GHSV_{(N.C.)} = 7000\,h^{-1}$, $v_L = 0.39\,mN\,s^{-1}$. Gas feed composition: [NO] = 0–500 ppm, [CH_4] = 1000 ppm, [O_2] = 5 vol.%, and [N_2] = balance.

with the characterisation results the best catalyst under these operating conditions for NO reduction was Pd–Cl/SA which has the highest amount of surface sulphate with accessible Lewis superacid sites and for which the CH_4 oxidation light-off temperatures was above 400 °C.

From the results shown in Fig. 7 for the methane oxidation in the absence of NO it may be observed that the light-off temperatures were much lower than those observed in its presence. This difference was attributed to the competitive adsorption between NO and CH_4 for the same Pd^{2+} active sites, where the stronger NO adsorption capacity causes a shift in the CH_4 light-off to higher temperatures and thus favours the SCR reaction.

It has been shown that the sulphation of alumina generates an increase in both the amount and strength of the acid sites [26]. These strong acid sites probably stabilise the Pd^{2+} species or dispersed PdO species as previously described for acidic zeolites [27–29]. On Pd/SZr, Pd^{2+} ions on acid sites are the active centres for the SCR of NO, while PdO clusters favour the combustion of CH_4 and thus decrease the NO conversion. Even starting on pre-reduced samples metallic Pd is rapidly transformed into Pd^{2+} ions when in contact with the reaction mixture. On non-acidic materials Pd particles are transformed into PdO clusters that are very active for methane oxidation [27,29]. From the results presented in this study considering the high NO conversions the presence of stabilised Pd^{2+} species on the sulphated alumina support is expected.

The Pd catalysts prepared on the alumina without acid pretreatment had a lower catalytic activity than the sulphated support, in agreement with previous results obtained for CoO/Al_2O_3 catalysts [16]. The Pd–Cl/SA catalysts developed in this work presented a better performance for NO reduction than those CoO_x/SA catalysts, reaching 70% conversion at 550 °C compared to only 50% for the analogous CoO_x/SA catalysts. The presence of nitric oxide favoured the formation of nitrate species with the cobalt catalysts that were directly related to the methane oxidation capacity and thus to the selectivity of the catalyst towards N_2. Thus, with the sulphated alumina supports studied here the higher methane oxidation activity observed for the catalyst prepared from the nitrate precursor could be also due to the formation of these nitrate species.

The low catalytic activity of the sample prepared from the acetate precursor could be attributed not only to the presence of multilayer sulphate species that inhibit access of the reactant gases to the active sites within the mesoporous structure but also to the lower activity of the $Al_2(SO_4)_3$ phase, known to be present from the XRD results. The catalyst produced from the chloride precursor had

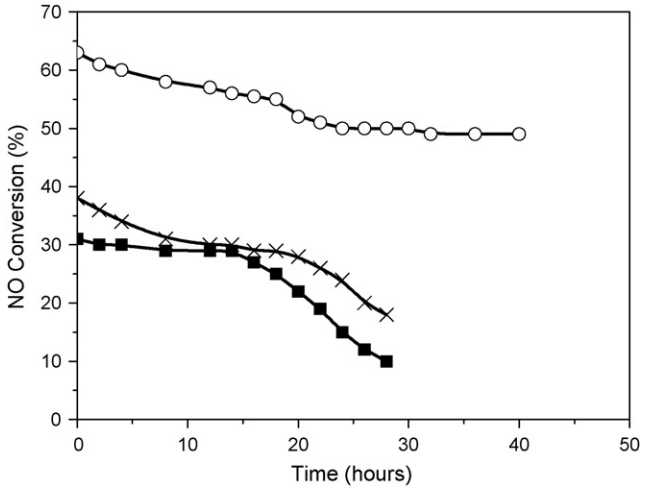

Fig. 8. Catalysts stability with reaction time, at the maximum NO conversion temperature: (◯) Pd–Cl/SA; (■) Pd–N/SA; (×) Pd–Ac/SA. Operating conditions: total flow $Q = 3500\ mL\ min^{-1}$, $P = 120\ kPa$, $GHSV_{(N.C.)} = 7000\ h^{-1}$, and $v_L = 0.39\ mN\ s^{-1}$. Gas feed composition: [NO] = 500 ppm, [CH_4] = 1000 ppm, [O_2] = 5 vol.%, and [N_2] = balance.

a lower methane oxidation activity, similar to that observed with the sample produced from the acetate precursor that presented a similar amount of Lewis acidity but much higher concentration of surface sulphates. The inhibition of the methane oxidation in the presence of NO for the catalyst produced from the chloride precursor was probably due to the interaction of this ion with the active phase. It has been previously proposed that chloride ions from the palladium precursor could migrate to the active Pd^{2+} centres under reaction conditions, blocking and inhibiting the methane oxidation [20]. Furthermore, the chloride could provide an additional acid character that favoured the NO reduction, although the most significant acidity in these catalysts was due to the strongly adsorbed sulphates that lead to the superacid character [23].

Concerning the role of NO_2 in these catalysts, several mechanisms have been proposed in the literature although the mechanism is still unclear. According to some authors the acidic sites facilitate the oxidation of NO to NO_2, which is the rate-determining step in the SCR of NO over Pd catalysts [30,31]. Other authors studying SCR with Pd loaded ZSM-5 zeolites have proposed that acid sites not only indirectly promoted the reaction by maintaining the high Pd dispersion but also directly participate in the oxidation of NO to NO_2 and the reduction of NO_2 to N_2 [3,32]. However, other authors working with Pd/SZ catalysts did not find evidence for the formation of NO_2 in Pd/SZ catalysts, while for Pd/sulphated Zr a low activity for the NO oxidation to NO_2 has been reported [33]. The absence of NO_2, N_2O or NH_3 as reaction products in the catalysts studied here could be related with the direct activation of NO over Pd^{2+} species or with the fast reaction of the $NO_{x(ads)}$ species with the C_xH_y species adsorbed on Pd^{2+} sites.

Decisive factors for the industrial use of any catalyst are the stability activity and selectivity under operating conditions. The catalytic activities of the three systems after 40 h in operation are shown in Fig. 8. From this figure it may be observed that the catalyst prepared from the chloride precursor salt not only lead to the highest catalytic activities but was also the most stable.

Thermogravimetric analyses of the catalysts after the SCR-CH_4 reduction reaction are shown in Fig. 9. Comparing this figure with that obtained for the fresh catalysts shown in Fig. 3 it may be appreciated that the weight losses associated with the loss of surface sulphates were similar for the Pd–Cl/SA catalyst but lower for the other two with a marked reduction in the case of Pd–Ac/SA, especially in the temperature range associated with the more weakly adsorbed surface sulphates. The results indicate that the stability

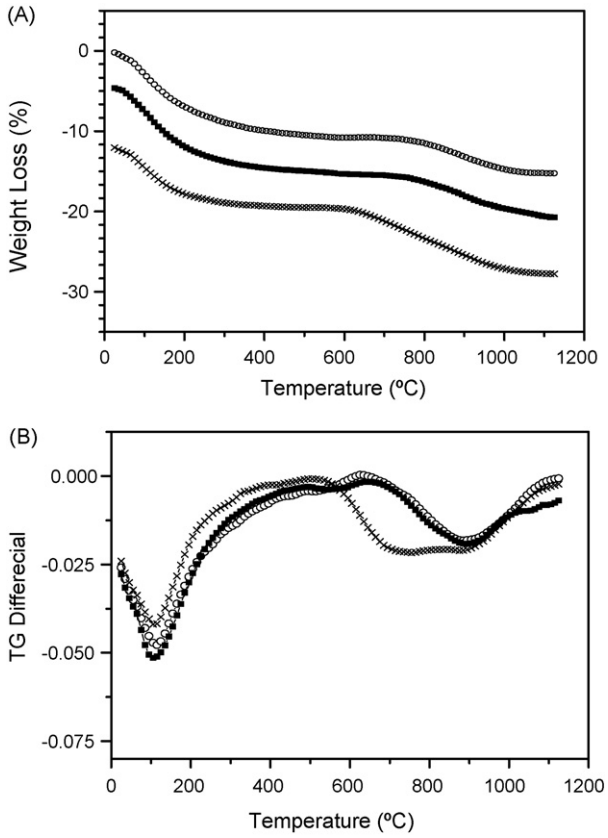

Fig. 9. TGA (A) and DTG (B) curves for the sulphated support and Pd catalysts after catalytic tests: (◯) Pd–Cl/SA; (■) Pd–N/SA; (×) Pd–Ac/SA.

of the PdCl/SA catalyst may be due to the presence of Cl^- ions that favour the stabilisation of the Pd^{2+} phase.

For the most active and stable catalyst (Pd–Cl/SA) the effect of water vapour (2 vol.%) in the reaction gases on the catalytic activity was studied at the maximum conversion temperature of 550 °C. When water was introduced into the gas mixture there was a steady decrease in the catalytic activity for 5 h until a constant value 20% lower than the original activity was reached. In contrast for the non-sulphated Pd–Cl/SA material the catalytic activity was completely suppressed. This reduction was probably due to the competitive adsorption of OH groups onto the active sites where the NO_x and CH_x species need to be adsorbed. After the steady state conditions were reached the NO conversion was constant for more than 10 h. When the addition of water vapour was stopped the original NO conversion value was achieved, indicating that no structural or chemical modification of the active species took place in the presence of water vapour.

4. Conclusions

Pretreatment with sulphuric acid of the conformed alumina monoliths leads to the incorporation of a number of different sulphate species. These species generate acid centres of different strengths and natures that control the adsorption of NO on the catalyst surface. The results showed that Pd species anchored on surface sulphate species, detected by the various techniques, were the active centres directly involved in the NO reduction with CH_4. Weakly anchored multilayer sulphate species on the catalysts surface inhibit the interaction of the reactants with the active sites, leading to catalysts with lower activities and stabilities. The Pd catalysts impregnated on the sulphated alumina had significantly higher catalytic activities for the reduction of NO with methane in

lean conditions than analogous Pd catalysts impregnated on alumina supports that had not been previously sulphated.

The palladium deposited from different precursor salts gave rise to different values in both activity and stability. For NO reduction with methane in excess oxygen the catalyst prepared from the chloride precursor gave rise to higher NO reduction values and negligible activity for the undesired competing methane oxidation reaction. In contrast, the catalyst produced from the nitrate precursor was extremely active for methane oxidation. Furthermore, the poor mechanical strengths of the samples produced with the nitrate and especially the acetate precursors made them unsuitable for practical use. Thus, the Pd–Cl/SA catalyst was the most active for CH_4-SCR of NO in oxygen excess while the Pd–N/SA catalyst could be used in processes where the concentrations of NO were relatively low but required the total elimination of trace methane from the system.

Acknowledgements

The authors would like to thank the Comunidad Autónoma of Madrid CAM project *GR/AMB/0751/2004SE505* and the Program "Ciencia y Tecnología para el Desarrollo" CYTED, Project V.7 for their financial support. Also to Dr. José Luis García Fierro for the TPR measurements.

References

[1] J.N. Armor, Catal. Today 26 (1995) 147.
[2] M.D. Fokema, J.Y. Ying, Catal. Rev. 43 (2001).
[3] M. Misono, Y. Nishizaka, M. Kawamoto, H. Kato, Stud. Surf. Sci. Catal. 105 (1997) 1501.
[4] N. Li, A. Wang, J. Tang, X. Wang, D. Liang, T. Zhang, Appl. Catal. B 43 (2003) 195.
[5] M. Iwamoto, H. Yahiro, Y. Yu-u, S. Shundo, N. Mizuno, Shokubai (Catalyst) 32 (1990) 430.
[6] H. Hamada, Y. Kintaichi, M. Sakai, T. Ito, M. Tabata, Appl. Catal. 64 (1990) L1.
[7] K. Arata, M. Hino, Appl. Catal. 59 (1990) 197.
[8] A. Wang, D. Liang, C. Xu, X. Sun, T. Zhang, Appl. Catal. B 32 (2001) 205.
[9] H. Ohtsuka, T. Tabata, Appl. Catal. B 29 (2001) 177.
[10] H. Hamada, Y. Kintaichi, M. Sakai, T. Ito, M. Tabata, Appl. Catal. 75 (1991) L1.
[11] R. Burch, A. Ramli, Appl. Catal. B 15 (1998) 49.
[12] G.R. Bamwenda, A. Obuchi, A. Ogata, J. Oi, S. Kushiyama, K. Mizuno, J. Mol. Catal. A: Chem. 126 (1997) 151.
[13] R. Long, R.T. Yang, Catal. Lett. 52 (1998) 91.
[14] C.J. Loughran, D.E. Resasco, Appl. Catal. B 7 (1995) 113.
[15] Y. Nishizaka, M. Misono, Chem. Lett. (1994) 2237.
[16] J.C. Martín, P. Ávila, S. Suarez, M. Yates, A.B. Martín-Rojo, C. Barthelemy, J.A. Martín, Appl. Catal. B 67 (2006) 270.
[17] L. Ning, W. Aiqin, Z. Mingyuan, W. Xiadong, Z. Tao, Chin. J. Catal. 24 (2003) 809.
[18] E.W. Washburn, Proc. Natl. Acad. Sci. U.S.A. 7 (1921) 115.
[19] J. Rouquerol, D. Avnir, C.W. Fairbridge, D.H. Everett, J.H. Haynes, N. Pericone, J.D.F. Ramsay, K.S.W. Sing, K.K. Unger, Pure Appl. Chem. 66 (1994) 1739.
[20] D. Roth, P. Gélin, M. Primet, E. Tena, Appl. Catal. A 203 (2000) 37.
[21] J.C. Martín, Ph.D. Thesis, Desarrollo de catalizadores estables basados en alúmina para la reducción de NO_x con hidrocarburos en condiciones oxidantes, 2007.
[22] M. Yates, J. Blanco, M.A. Martin-Luengo, M.P. Martin, Micropor. Mesopor. Mater. 65 (2003) 219.
[23] T.-s. Yang, T.-s. Chang, T.-t. Yeh, J. Mol. Catal. A: Chem. 115 (1997) 339.
[24] V. Ferrer, A. Moronta, J. Sánchez, R. Solano, S. Bernal, D. Finol, Catal. Today 107–108 (2005) 487.
[25] H. Lieske, J. Volter, J. Phys. Chem. 89 (1985) 1841.
[26] N. Li, A. Wang, L. Li, X. Wang, L. Ren, T. Zhang, Appl. Catal. B 50 (2004) 1.
[27] Y.-H. Chin, W.E. Alvarez, D.E. Resasco, Catal. Today 62 (2000) 159.
[28] A.W. Aylor, L.J. Lobree, J.A. Reimer, A.T. Bell, J. Catal. 172 (1997) 453.
[29] Y.-H. Chin, A. Pisanu, L. Serventi, W.E. Alvarez, D.E. Resasco, Catal. Today 54 (1999) 419.
[30] M. Ogura, Y. Sugiura, M. Hayashi, E. Kikuchi, Catal. Lett. 42 (1996) 185.
[31] H. Kato, C. Yokoyama, M. Misono, Catal. Lett. 47 (1997) 189.
[32] H. Kato, C. Yokoyama, M. Misono, Catal. Today 45 (1998) 93.
[33] H. Ohtsuka, Appl. Catal. B 33 (2001) 325.